

Thermal QCD Deconfinement Phase Transition in a Finite Volume within the Color-Singletness Condition

M. Ladrem, A. Ait-El-Djoudi and G. Yezza

Laboratoire de Physique des Particules et Physique Statistique

Ecole Normale Supérieure-Kouba,

B.P. 92, 16050, Vieux-Kouba, Algiers, Algeria.

E-mail: *Ladrem@eepad.dz, Aitamel@eepad.dz*

(Dated: February 1, 2008)

Abstract. We study the finite size effects on the thermal deconfinement phase transition from the hadronic gas phase to the QGP phase, using a simple thermodynamic model based on the coexistence of confined and deconfined phases in a finite volume. We first consider the bag model partition function for the QGP, then we include the necessary color singletness condition. By probing the behavior of some physical quantities on the hole range of temperature, it turns out that in a finite size system, all singularities occurring in these quantities in the thermodynamic limit ($V \rightarrow \infty$) are smoothed out, and the phase transition is then rounded over a broadened critical region , with an additional shifting effect of the critical point induced by the exact color singletness requirement. An analysis of the finite size scaling behavior at criticality of some characteristic quantities allows us to determine the scaling critical exponents characterizing the thermal deconfinement phase transition. The obtained results are in good agreement with those predicted by other studies for a first-order phase transition.

1. INTRODUCTION

It is generally believed that at sufficiently high temperatures and/or densities a new phase of matter called the Quark Gluon Plasma (QGP) can be created. This is logically a consequence of the quark-parton level of the matter structure and of the dynamics of strong interactions described by the Quantum Chromo Dynamics (QCD) theory. Its existence, however, has been partly supported by Lattice QCD (LQCD) calculations and the Cosmological Standard Model predictions. Experimentally, the only way to study the QCD Deconfinement Phase Transition (DPT) occurring between the hadronic and QGP phases is to try to recreate, in Ultra Relativistic Heavy Ion Collisions (URHIC), conditions similar to those which occurred in the early times of the universe ($\sim 10^{-6} s$), immediately after the big bang.

If the QGP phase is (will be) created in URHIC at SPS (LHC and RHIC) colliders, the volume

in which it takes (will take) place is certainly finite. Also, in LQCD studies, the scale of the lattice space volume is finite. This is our motivation to study the Finite Size Effects (FSE) on the expected DPT from a Hadronic Gas (HG) phase to a QGP phase. These effects are certainly important since statistical fluctuations in a finite volume can hinder a sharp transition between the two phases. Only in the Thermodynamic Limit (TL) are phase transitions characterized by some singularities: δ -singularities for a discontinuous PT and power-law singularities for a continuous PT. In general, in finite systems, Finite Size Effects (FSE) lead to a rounding of these singularities and a possible mixing of phases. However, even in such a situation, it is possible to obtain informations on the critical behavior. Large but finite systems show a *universal* behavior called “Finite-Size Scaling” (FSS) allowing the put of all the physical systems undergoing a phase transition in a certain number of universality classes. The systems in a given universality class display the same critical behavior, meaning that certain dimensionless quantities have the same values for all these systems. *Critical exponents* are an example of these universal quantities.

In the present work, we study the FSE on the thermal QCD DPT, using a simple thermodynamic model based on the coexistence of the HG and QGP phases in a finite volume, with low energy density phase and high energy density phase equations of state [1]. For the HG phase, we have calculated the Partition Function (PF) of a pionic gas as a first approximation, and for the QGP phase, we have calculated the PF of a free gas of quarks and gluons. This latter is first derived simply within the bag model, then we include the exact color-singletness condition, since the color confinement phenomenon requires that the QGP phase must have a neutral color charge. This condition is implemented into the quantum statistical description of the system using the Group Theoretical Projection Technique (GTPT) [2]. This Color Singlet Partition Function (CSPF) can not be exactly calculated and is usually calculated within the saddle point and gaussian approximations in the limit $VT^3 \gg 1$ [3]. It turned out that the use of the such obtained PF, within the Phase Coexistence Model (PCM), has as a consequence the absence of the DPT [4]. This is due to the fact that the approximations used for the standard calculation of the CSPF, break down at $VT^3 \ll 1$, and this limit is attained using the PCM. We propose then a new method for calculating a suitable CSPF, containing an expansion in a power series of the QGP volume fraction, using the saddle point approximation but avoiding the problem arising at $VT^3 \ll 1$. The CSPF derived in this way allows us to accurately calculate physical quantities describing well the DPT at finite volumes, like the order parameter, the energy density and the entropy density, and probe the behavior of the PT at criticality. We show that in the TL, these thermodynamic quantities exhibit a discontinuity at a critical temperature $T_c(\infty)$, which appears as a delta function singularity in the first derivatives, i. e. in the specific heat and the susceptibility. In a finite size system, the discontinuities disappear and the variations of these quantities are perfectly

smooth over the hole range of temperature. The delta singularities are smeared into finite peaks of width $\delta T(V)$, which is nothing but the broadening of the critical region, with the maxima of the peaks occuring at an effective transition temperature $T_c(V)$ shifted away from the true critical temperature $T_c(\infty)$. This additional shifting effect of the critical temperature is induced by the exact color singleness requirement. An analysis of the FSS behavior at criticality of these maxima as well as of the width of the transition region and the shift of the effective transition temperature $T_c(V)$ relative to the true one $T_c(\infty)$ allows us to determine the scaling critical exponents characterizing the thermal QCD DPT.

2. THE QCD DECONFINEMENT PHASE TRANSITION IN A FINITE VOLUME

2.1. Phase Coexistence Model and Partition Functions Calculation

To study the QCD DPT in a finite volume, we consider a simple PCM used in [1], in which the mixed HG-QGP phase system has a finite volume: $V = V_{HG} + V_{QGP}$. The parameter \mathfrak{h} representing the fraction of volume occupied by the HG: $V_{HG} = \mathfrak{h}V$, is then defined and can be considered as an order parameter for the DPT. The value: $\mathfrak{h} = 1$ corresponds then to a total HG phase and when $\mathfrak{h} = 0$, the system is completely in the QGP phase. Assuming non-interacting phases (separability of the energy spectra of the two phases), the total Partition Function (PF) of the system can be approximatively written as:

$$Z(\mathfrak{h}) = Z_{QGP}(\mathfrak{h}) Z_{HG}(\mathfrak{h}). \quad (1)$$

The mean value of any thermodynamic quantity $A(T, \mu, V)$ of the system, as defined in [1], can then be calculated by:

$$\langle A(T, \mu, V) \rangle = \frac{\int_0^1 A(\mathfrak{h}) Z(\mathfrak{h}) d\mathfrak{h}}{\int_0^1 Z(\mathfrak{h}) d\mathfrak{h}}, \quad (2)$$

where $A(\mathfrak{h})$ is the total thermodynamic quantity in the state \mathfrak{h} , given in the case of an extensive quantity by:

$$\mathcal{A}(\mathfrak{h}) = \mathcal{A}_{HG}(T, \mathfrak{h}V) + \mathcal{A}_{QGP}(T, \mu, (1 - \mathfrak{h})V), \quad (3)$$

and in the case of an intensive quantity, by:

$$\mathcal{A}(\mathfrak{h}) = \mathfrak{h}\mathcal{A}_{HG}(T, \mathfrak{h}V) + (1 - \mathfrak{h})\mathcal{A}_{QGP}(T, \mu, (1 - \mathfrak{h})V), \quad (4)$$

with A_{QGP} and A_{HG} the thermodynamic quantities relative to the individual QGP and HG phases, respectively.

The partition functions of both HG and QGP phases are calculated, and their final expressions are given in the following. For a pionic gas, the PF is simply given by:

$$Z_{HG} = e^{\frac{\pi^2}{30}T^3V_{HG}}, \quad (5)$$

and for a QGP consisting of gluons and two flavors of massless quarks, with a chemical potential μ , within the bag model, the PF is given by [5]:

$$Z_{QGP} = \exp \left(\left(\frac{37\pi^2}{90}T^3 + \mu^2 T + \frac{1}{2\pi^2} \frac{\mu^4}{T} - \frac{B}{T} \right) V_{QGP} \right), \quad (6)$$

where B is the bag constant, accounting for the real vacuum pressure exercised on the perturbative vacuum.

2.2. Finite Size Effects on the DPT

We'll study in the following the FSE on the thermal QCD DPT, at a vanishing chemical potential ($\mu = 0$), and for this purpose, we'll examine the behavior of some thermodynamic quantities with temperature for varying volume. The quantities of interest are the order parameter, which is simply in this case the hadronic volume fraction $\mathfrak{h}(T, \mu, V)$, the entropy density $s(T, \mu, V)$ and the energy density $\varepsilon(T, \mu, V)$. Their mean values are calculated from eq.(2), and are given by the expressions:

$$\langle \mathfrak{h}(T, \mu, V) \rangle = \frac{(fV - 1)e^{fV} + 1}{fV(e^{fV} - 1)} \quad (7)$$

$$\begin{aligned} \langle s(T, \mu, V) \rangle &= \mathfrak{s}_{QGP} + (\mathfrak{s}_{HG} - \mathfrak{s}_{QGP}) \langle \mathfrak{h}(T, \mu, V) \rangle \\ \langle \varepsilon(T, \mu, V) \rangle &= \mathfrak{e}_{QGP} + (\mathfrak{e}_{HG} - \mathfrak{e}_{QGP}) \langle \mathfrak{h}(T, \mu, V) \rangle, \end{aligned} \quad (8)$$

with:

$$\begin{cases} f = \left(\frac{\pi^2}{30} - \frac{37\pi^2}{90} \right) T^3 - \mu^2 T - \frac{1}{2\pi^2} \frac{\mu^4}{T} + \frac{B}{T} \\ \mathfrak{s}_{QGP} = \frac{74\pi^2}{45} T^3 + 2\mu^2 T; \mathfrak{s}_{HG} = \frac{2\pi^2}{15} T^3 \\ \mathfrak{e}_{QGP} = B + \frac{37\pi^2}{30} T^4 + \mu^2 T^2 - \frac{\mu^4}{2\pi^2}; \mathfrak{e}_{HG} = \frac{\pi^2}{10} T^4. \end{cases} \quad (9)$$

Fig.(1) shows the three-dimensional plots of the order parameter, the normalized energy density $\frac{\langle \varepsilon(T, V) \rangle}{T^4}$, and the normalized entropy density $\frac{\langle s(T, V) \rangle}{T^3}$, vs temperature and system volume, at a vanishing chemical potential ($\mu = 0$), using the common value $B^{1/4} = 145\text{MeV}$ for the bag constant. The first-order character of the transition is showed by the step-like rise or sharp discontinuity of the illustrated quantities, approaching the TL, at a critical temperature $T_c(\infty) \simeq 104.5\text{MeV}$, which

reflects the existence of a latent heat accompanying the PT. The quantities $\frac{\langle \varepsilon \rangle}{T^4}$ and $\frac{\langle s \rangle}{T^3}$ are traditionally interpreted as a measure of the number of effective degrees of freedom; the temperature increase causes then a “melting” of the constituent degrees of freedom “frozen” in the hadronic state, making the energy and entropy densities attain their plasma values. In finite systems, the phase transition is rounded since the probability of presence of the QGP phase below T_c , and that of the HG phase above T_c are finite because of the considerable thermodynamical fluctuations. The transition region around the critical temperature $T_c(\infty)$ is then broadened, acquiring a bigger width, smaller is the volume.

3. THE QCD DPT IN A FINITE VOLUME INCLUDING THE COLOR-SINGLETNESS CONDITION

3.1. The Color-Singlet Partition Function of the QGP

The partition function for a color-singlet quark-gluon plasma contained in a volume V_{QGP} , at temperature T and quark chemical potential μ , is determined using the Group Theoretical Projection Technique (GTPT) formulated by Turko and Redlich [2] and is given by [3]:

$$Z_{QGP}(T, \mu, V_{QGP}) = \frac{8}{3\pi^2} e^{-\frac{BV_{QGP}}{T}} \int_{-\pi}^{+\pi} \int_{-\pi}^{+\pi} d\left(\frac{\varphi}{2}\right) d\left(\frac{\psi}{3}\right) M(\varphi, \psi) \tilde{Z}(T, \mu, V_{QGP}; \varphi, \psi), \quad (10)$$

where $M(\varphi, \psi)$ is the weight function (Haar measure) given by:

$$M(\varphi, \psi) = \left(\sin\left(\frac{1}{2}(\psi + \frac{\varphi}{2})\right) \sin\left(\frac{\varphi}{2}\right) \sin\left(\frac{1}{2}(\psi - \frac{\varphi}{2})\right) \right)^2, \quad (11)$$

and \tilde{Z} the generating function defined by:

$$\tilde{Z}(T, \mu, V_{QGP}; \varphi, \psi) = Tr \left[\exp \left(-\beta \left(\hat{H}_0 - \mu(\hat{N}_q - \hat{N}_{\bar{q}}) \right) + i\varphi \hat{I}_3 + i\psi \hat{Y}_8 \right) \right], \quad (12)$$

where $\beta = \frac{1}{T}$ with the units chosen as: $k_B = \hbar = c = 1$, \hat{H}_0 is the free quark-gluon Hamiltonian, \hat{N}_q ($\hat{N}_{\bar{q}}$) denotes the (anti-) quark number operator, and \hat{I}_3 and \hat{Y}_8 are the color “isospin” and “hypercharge” operators respectively.

The generating function $\tilde{Z}(T, V_{QGP}, \mu; \varphi, \psi)$ can be factorized into the quark contribution and the gluon contribution as:

$$\tilde{Z}(T, \mu, V_{QGP}; \varphi, \psi) = \tilde{Z}_{quark}(T, \mu, V_{QGP}; \varphi, \psi) \tilde{Z}_{gluon}(T, V_{QGP}; \varphi, \psi), \quad (13)$$

where the quark contribution is given by:

$$\tilde{Z}_{quark}(T, \mu, V_{QGP}; \varphi, \psi) = \exp \left[\frac{\pi^2}{12} T^3 V_{QGP} d_Q \sum_{q=r,g,b} \left(\frac{7}{30} - \left(\frac{\alpha_q - i(\frac{\mu}{T})}{\pi} \right)^2 + \frac{1}{2} \left(\frac{\alpha_q - i(\frac{\mu}{T})}{\pi} \right)^4 \right) \right], \quad (14)$$

with $q = r, b, g$ the color indices, $d_Q = 2N_f$ counts the spin-isospin degeneracy of quarks and the angles α_q being determined by the eigenvalues of the color charge operators in eq. (12):

$$\alpha_r = \frac{\varphi}{2} + \frac{\psi}{3}, \quad \alpha_g = -\frac{\varphi}{2} + \frac{\psi}{3}, \quad \alpha_b = -\frac{2\psi}{3}, \quad (15)$$

and the gluon contribution is given by:

$$\tilde{Z}_{gluon}(T, V_{QGP}; \varphi, \psi) = \exp \left[\frac{\pi^2}{12} T^3 V_{QGP} d_G \sum_{g=1}^4 \left(-\frac{7}{30} + \left(\frac{\alpha_g - \pi}{\pi} \right)^2 - \frac{1}{2} \left(\frac{\alpha_g - \pi}{\pi} \right)^4 \right) \right], \quad (16)$$

with $d_G = 2$ the degeneracy factor of gluons and α_g ($g = 1, \dots, 4$) being:

$$\alpha_1 = \alpha_r - \alpha_g, \quad \alpha_2 = \alpha_g - \alpha_b, \quad \alpha_3 = \alpha_b - \alpha_r, \quad \alpha_4 = 0. \quad (17)$$

Let us write eq. (10) on the form:

$$Z_{QGP}(T, \mu, V_{QGP}) = \frac{8}{3\pi^2} e^{qV(T^3 g_0(\frac{\mu}{T}) - \frac{B}{T})} \int_{-\pi}^{+\pi} \int_{-\pi}^{+\pi} d(\frac{\varphi}{2}) d(\frac{\psi}{3}) M(\varphi, \psi) e^{(g(\varphi, \psi, \frac{\mu}{T}) - g_0(\frac{\mu}{T}))qVT^3}, \quad (18)$$

with:

$$\begin{aligned} g(\varphi, \psi, \frac{\mu}{T}) &= \frac{\pi^2}{12} \left(\frac{21}{30} d_Q + \frac{16}{15} d_G \right) + \frac{\pi^2}{12} \frac{d_Q}{2} \sum_{q=r,b,g} \left\{ -1 + \left(\frac{(\alpha_q - i(\frac{\mu}{T}))^2}{\pi^2} - 1 \right)^2 \right\} \\ &\quad - \frac{\pi^2}{12} \frac{d_G}{2} \sum_{g=1}^4 \left(\frac{(\alpha_g - \pi)^2}{\pi^2} - 1 \right)^2, \end{aligned} \quad (19)$$

$g_0(\frac{\mu}{T})$ being the maximum of $g(\varphi, \psi, \frac{\mu}{T})$ for $\varphi, \psi \in [-\pi, +\pi]$, given as:

$$g_0(\frac{\mu}{T}) = \frac{\pi^2}{12} \left(\frac{21}{30} d_Q + \frac{16}{15} d_G \right) + \frac{\pi^2 d_Q}{12} \left(\frac{3\mu^2}{\pi^2 T^2} + \frac{3\mu^4}{2\pi^4 T^4} \right), \quad (20)$$

and q the QGP volume fraction: $q = 1 - h$.

We evaluate the integral in eq. (18) by expanding M to leading order in φ and ψ , and g to fourth order in φ and ψ . Concerning the two terms appearing from g , we do an expansion of the part depending on the volume to second order for $VT^3 \gg 1$, while the term independent of the volume is expanded in a series on the form [4]:

$$e^{\mathcal{D}(\varphi, \psi)q} = \sum_{j=0}^{\infty} \frac{(\mathcal{D}(\varphi, \psi))^j}{j!} q^j. \quad (21)$$

After some calculation, the final color-singlet partition function of the QGP, Z_{QGP} , can then be expressed as [6]:

$$Z_{QGP}(T, \mu, Vq) \simeq \frac{4}{9\pi^2} \frac{e^{qV(T^3 g_0(\frac{\mu}{T}) - \frac{B}{T})}}{\left(a(\frac{\mu}{T}) VT^3 \right)^4} \left[\sum_{n=0}^{\infty} I_{n0} q^n - \frac{7}{12\pi^2 a^2(\frac{\mu}{T}) VT^3} \sum_{p=0}^{\infty} I_{p1} q^{p+1} \right], \quad (22)$$

where the general form of the integral coefficients I_{nm} is given by:

$$I_{nm} = \int_{-\pi}^{\pi} \int_{-\pi}^{\pi} d\varphi d\psi M^{(0,0)}(\varphi, \psi) (n!)^{-1} \left(-\frac{2}{3} \left(\varphi^2 + \frac{4}{3}\psi^2 \right) \right)^n \left(\frac{\varphi^4}{8} + \frac{2\psi^4}{9} + \frac{\varphi^2\psi^2}{3} \right)^m, \quad (23)$$

with: $a(\frac{\mu}{T}) = \left(\frac{d_Q}{16} \left(\frac{3\mu^2}{\pi^2 T^2} + 1 \right) + \frac{3}{8} d_G \right)$, $M^{(0,0)}$ being the expansion of M to leading order in φ and ψ .

3.2. Finite Size Effects

The mean values of the order parameter, the energy and entropy densities can also be computed in this case, using the obtained CSPF within the definition (2). Their expressions for two quark flavors are respectively given by:

$$\langle \mathfrak{h}(T, \mu, V) \rangle_{\text{csc}} = 1 - \frac{\int_0^1 d\mathfrak{q} e^{\tilde{f}V\mathfrak{q}} \left(\sum_{n=0}^{\infty} I_{n0}\mathfrak{q}^{n+1} - \frac{7 \sum_{p=0}^{\infty} I_{p1}\mathfrak{q}^{p+2}}{12\pi^2 a^2 (\frac{\mu}{T}) VT^3} \right)}{\int_0^1 d\mathfrak{q} e^{\tilde{f}V\mathfrak{q}} \left(\sum_{n=0}^{\infty} I_{n0}\mathfrak{q}^n - \frac{7 \sum_{p=0}^{\infty} I_{p1}\mathfrak{q}^{p+1}}{12\pi^2 a^2 (\frac{\mu}{T}) VT^3} \right)} \quad (24)$$

$$\langle \varepsilon(T, \mu, V) \rangle_{\text{csc}} = \mathfrak{e}_{QGP} + \mathfrak{e}_0 + (\mathfrak{e}_{HG} - \mathfrak{e}_{QGP}) \langle \mathfrak{h}(T, \mu, V) \rangle_{\text{csc}} \quad (25)$$

$$\langle s(T, \mu, V) \rangle_{\text{csc}} = \mathfrak{s}_{QGP} + \mathfrak{s}_0 + (\mathfrak{s}_{HG} - \mathfrak{s}_{QGP}) \langle \mathfrak{h}(T, \mu, V) \rangle_{\text{csc}}, \quad (26)$$

with:

$$\begin{cases} \tilde{f}(T, \mu) = \left(\left(\frac{\pi^2}{30} + g_0(\frac{\mu}{T}) \right) T^3 - \frac{B}{T} \right) \\ \mathfrak{e}_0 = -12\frac{T}{V} ; \mathfrak{s}_0 = -\frac{12}{V} - \frac{4}{V} \ln \left(VT^3 a \left(\frac{\mu}{T} \right) \right), \end{cases} \quad (27)$$

$g_0(\frac{\mu}{T})$ and $a(\frac{\mu}{T})$ being taken for $N_f = 2$.

Fig. (2) illustrates as in the previous section the variations of the above quantities with temperature for different system sizes, but in this case including the necessary condition of color-singletness for the QGP. Additionally to the rounding of the transition in geometrically finite systems, the color singletness requirement causes a shift of the critical temperature to higher values, when the volume decreases. The internal degrees of freedom being gradually “frozen” with decreasing volume, the pressure of the color-singlet QGP, related to the energy density by the well known relation: $P_{QGP} = \frac{1}{3}(\mathfrak{e}_{QGP} - 4B)$, is lower at a given temperature, and the mechanical Gibbs equilibrium between the two phases would then be reached for $T_c(V) > T_c(\infty)$. For small size systems, the transition is then smoothed out over a range of temperature $\delta T(V)$, around an effective transition temperature $T_c(V)$, shifted from the true transition temperature $T_c(\infty)$.

4. FINITE-SIZE SCALING ANALYSIS

4.1. Finite-Size Scaling

In the TL, phase transitions are characterized by the appearance of singularities in some second derivatives of the thermodynamic potential, such as the susceptibility χ and the specific heat c .

For a first order phase transition, the divergences are δ -function singularities, corresponding to the discontinuities in the first derivatives of the thermodynamic potential. For instance, in the case of the thermal QCD DPT, the δ -singularities appear in the susceptibility $\chi(T, V)$, defined to be the first derivative of the order parameter with respect to temperature, i. e., $\chi(T, V) = \frac{\partial \langle h(T, V) \rangle}{\partial T}$, and in the specific heat density $c(T, V)$ defined as: $c(T, V) = \frac{\partial \langle \varepsilon(T, V) \rangle}{\partial T}$. In finite volumes, these δ -functions are rounded into finite peaks over a range of temperature $\delta T(V)$ as illustrated in Fig. (3), and the peaks occurring at an effective transition temperature $T_c(V)$ are shifted away from the true critical temperature $T_c(\infty)$. The width of the transition region, the shift of the critical temperature and the maxima of the peaks of the specific heat and the susceptibility show a scaling behavior at criticality, characterized by scaling critical exponents as:

$$\left\{ \begin{array}{l} \delta T(V) \sim V^{-\theta_T} \\ \tau_T(V) = T_c(V) - T_c(\infty) \sim V^{-\lambda_T} \\ c_T^{\max}(V) \sim V^{\alpha_T} \\ \chi_T^{\max}(V) \sim V^{\gamma_T}. \end{array} \right. \quad (28)$$

The finite size scaling (FSS) analysis is used to recover the scaling critical exponents, and it has been shown [7] that for a first order phase transition, the finite size quantities $\delta T(V)$, $\tau_T(V)$ scale as: V^{-1} , and the maxima $c_T^{\max}(V)$ and $\chi_T^{\max}(V)$ scale as: V . The critical exponents θ_T , λ_T , γ_T and α_T are then all equal to unity.

4.2. Numerical determination of the scaling critical exponents for the thermal QCD DPT

4.2.1. The susceptibility scaling critical exponent γ_T

The plots of the susceptibility are presented in Fig.(4-left) versus temperature for various sizes. The delta function singularity of the susceptibility occurring in the TL is smeared, in a finite volume, into a finite peak of width $\delta T(V)$, with the maximum of the peak $|\chi_T|^{\max}(V)$ occurring at the effective transition temperature $T_c(V)$. The plot of the maxima $|\chi_T|^{\max}(V)$ versus volume is illustrated in Fig.(4-right), and the linearity of the data with V can clearly be noted. A numerical parametrization with the power-law form: $|\chi_T|^{\max}(V) \sim V^{\gamma_T}$, gives the value of the susceptibility critical exponent: $\gamma_T = 0.99 \pm 0.04$. Let us note that the associated error is a systematic one, resulting from the errors in the localization of the maxima. This systematic error will be estimated for all the critical exponents determined in the following.

4.2.2. The specific heat scaling critical exponent α_T

The variations with temperature of the specific heat density are presented for different sizes in Fig.(5-left), which shows the rounding of the delta function singularity of $c(T, V)$ in finite systems into a finite peak of width $\delta T(V)$ and height $c_T^{\max}(V)$. For decreasing volume, the width gets larger while the height of the peak decreases. The data of the maxima of the specific heat $c_T^{\max}(V)$ are fitted to the power-law form: $c_T^{\max}(V) \sim V^{\alpha_T}$ in Fig.(5-right), and the obtained specific heat critical exponent is: $\alpha_T = 0.99 \pm 0.04$.

4.2.3. The shift scaling critical exponent λ_T

For the study of the shift of the transition temperature $\tau_T(V) = T_c(V) - T_c(\infty)$, we need to have the finite size transition temperature $T_c(V)$. This latter is defined to be the temperature at which the rounded peaks of the susceptibility and the specific heat reach their maxima, and is found to be shifted away from the true transition temperature $T_c(\infty)$. Fig.(6) illustrates the results for the shift of the transition temperature plotted versus inversed volume, and shows the linear character of the variations. The shift critical exponent obtained from a fit to the form: $\tau_T(V) \sim V^{-\lambda_T}$, is: $\lambda_T = 1.0085 \pm 0.0009$.

4.2.4. The smearing scaling critical exponent θ_T

The width of the transition region can be defined by the gap: $\delta T(V) = T_2(V) - T_1(V)$ with $T_1(V)$ and $T_2(V)$ the temperatures at which the second derivative of the order parameter reaches its maxima, or in other terms the temperatures at which the third derivative of the order parameter vanishes, i. e., $\frac{\partial^3}{\partial T^3} \langle h(T, V) \rangle \Big|_{T_1(V), T_2(V)} = 0$.

Fig.(7-left) illustrates the variations of the second derivative of the order parameter with temperature for various sizes, and shows that the gap between the two extrema, which represents the broadening of the transition region, decreases with increasing volume. The results for the widths $\delta T(V)$, plotted in Fig.(7-right) vs the inverse of the volume, were fitted to the power law form: $\delta T(V) \sim V^{-\theta_T}$, and the obtained smearing critical exponent is: $\theta_T = 1.016 \pm 0.007$.

5. CONCLUSION

Our work has shown the influence of the finiteness of the system size on the behavior of thermodynamical quantities near criticality. The sharp transition observed in the thermodynamical limit,

signaled by discontinuities in the order parameter and in the energy and entropy densities at a critical temperature $T_c(\infty)$, is rounded off in finite volumes, and the variations of these thermodynamic quantities are perfectly smooth on the hole range of temperature. All discontinuities are rounded over a broadened critical region of width $\delta T(V)$ around the critical temperature, and the delta function singularities corresponding to these discontinuities, appearing in the first derivatives of these quantities, i.e. in the susceptibility and specific heat density, are then rounded into finite peaks of widths $\delta T(V)$. The inclusion of the exact color-singletness requirement in the QGP partition function induces an additionnal shifting effect of the effective transition temperature $T_c(V)$ to higher values ($T_c(V) > T_c(\infty)$). A FSS analysis of the behavior of the width of the transition region $\delta T(V)$, the shift of the effective transition temperature relative to the true one $\tau_T(V) = T_c(V) - T_c(\infty)$, and the maxima of the rounded peaks of the susceptibility $\chi_T^{\max}(V)$ and the specific heat $c_T^{\max}(V)$ near criticality, shows their power-law variations with the volume characterized by the scaling critical exponents θ_T , λ_T , α_T , γ_T . Numerical results for these critical exponents have been obtained, and the associated systematic errors, resulting from the numerical method used for the localization of the maxima $\chi_T^{\max}(V)$ and $c_T^{\max}(V)$ and of $T_1(V)$ and $T_2(V)$, have been estimated. These numerical values are in good agreement with our analytical results: $\theta_T = \lambda_T = \alpha_T = \gamma_T = 1$ obtained in a parallel work [8]. These results are characteristic of the first order phase transition, as predicted by different FSS theoretical approaches [9].

- [1] C. Spieles, H. Stöcker and C. Greiner, Phys. Rev. **C57** (1998) 908.
- [2] K. Redlich and L.Turko, Z. Phys. **C5** (1980) 201; L.Turko, Phys. Lett. **104B** (1981) 153.
- [3] H.-Th. Elze, W. Greiner and J. Rafelski , Phys. Lett. **124B** (1983) 515; Zeit. Phys. **C24** (1984) 361; H.-Th. Elze and W. Greiner, Phys. Lett. **179B** (1986) 385.
- [4] G. Yezza, Magister thesis in theoretical physics, Ecole Normale Supérieure-Kouba, Algiers (March 2002).
- [5] A. Ait-El-Djoudi, Magister thesis in theoretical physics, Ecole Normale Supérieure-Kouba, Algiers (October 1999).
- [6] M. Ladrem, A. Ait-El-Djoudi and G. Yezza, hep-ph/0207367; communication at the international conference Quark Matter 2002, held in Nantes-France from 18 to 24 July 2002.
- [7] K. Binder and D. W. Heermann, *Monte Carlo Simulations in Statistical Physics*, (Springer-Verlag, 2002).
- [8] M. Ladrem, A. Ait-El-Djoudi and G. Yezza, communication at the international conference ‘Quark Confinement and the Hadron spectrum’, held in Gargnano-Italy from 10 to 14 September 2002.
- [9] J. G. Brankov, D. M. Danchev and N. S. Tonchev, *Theory of Critical Phenomena in Finite-Size Systems - Scaling and Quantum Effects*, (World Scientific).

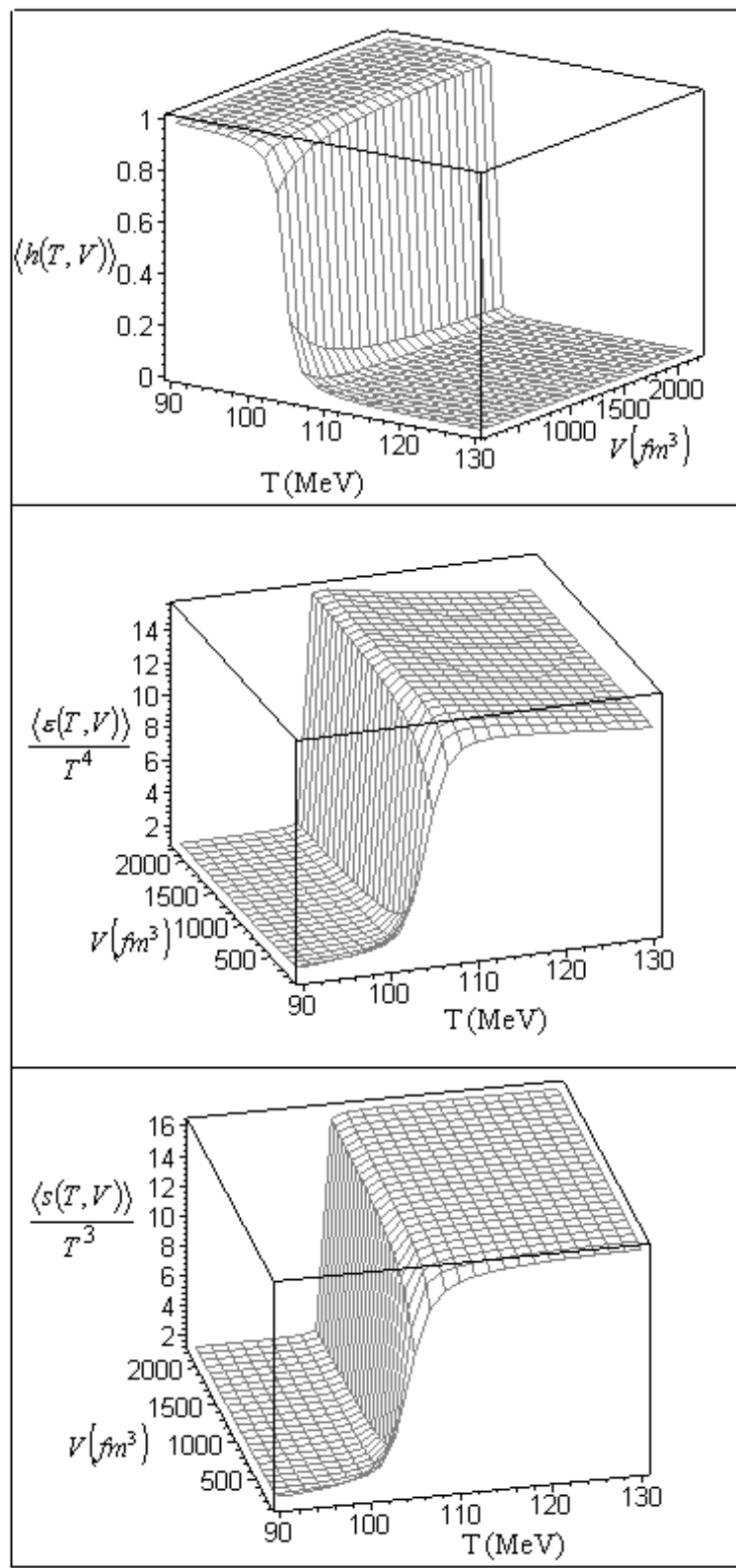


Fig. 1: Three dimensional plots of the mean values of (top) the order parameter, (middle) the energy density normalized by T^4 and (bottom) the entropy density normalized by T^3 , with temperature T and system size V , at $\mu = 0$.

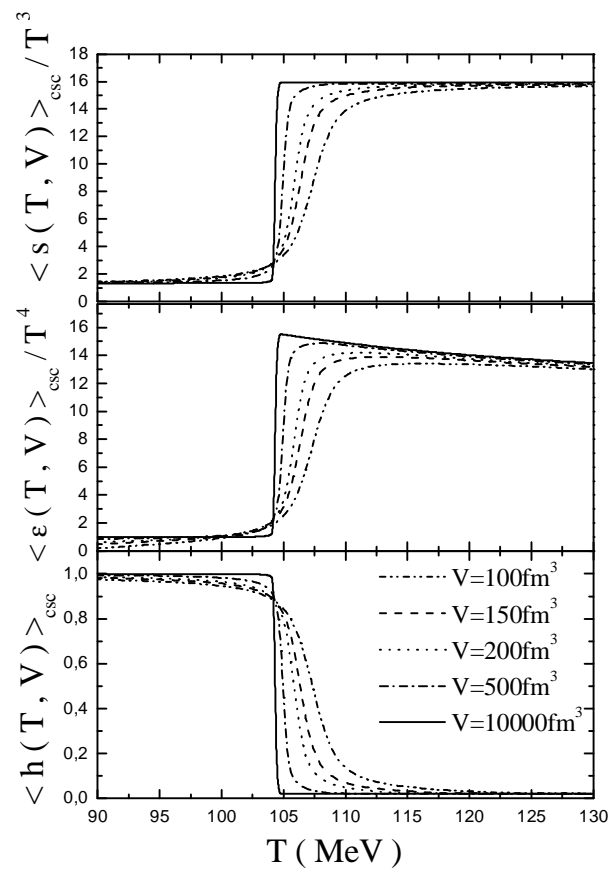


Fig. 2: Plots of (bottom) order parameter, (middle) energy density normalized by T^4 and (top) entropy density normalized by T^3 versus temperature at $\mu = 0$, for different system sizes including the color-singletness condition.

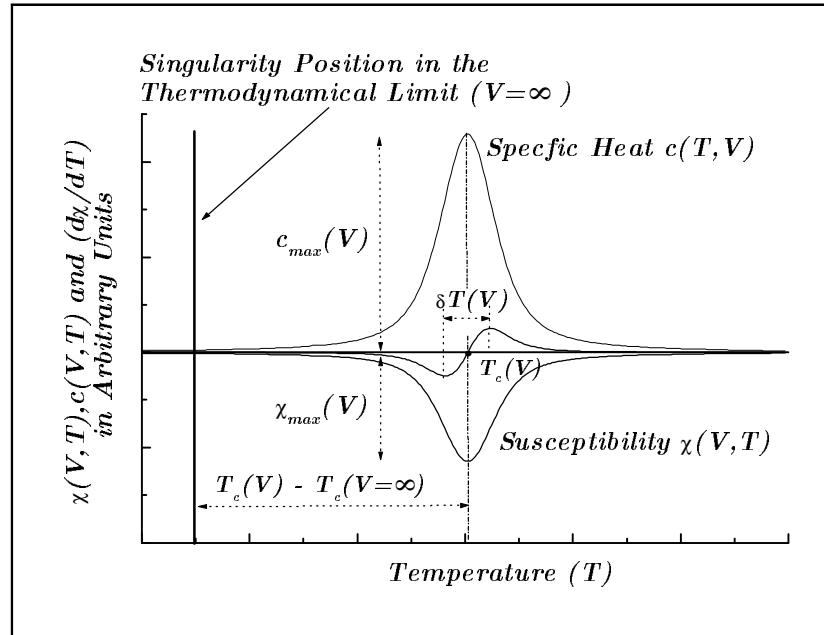


Fig. 3: Illustration of the critical behavior of the susceptibility $\chi(T, V)$, the specific heat $c(T, V)$ and the second derivative of the order parameter $\partial\chi/\partial T$.

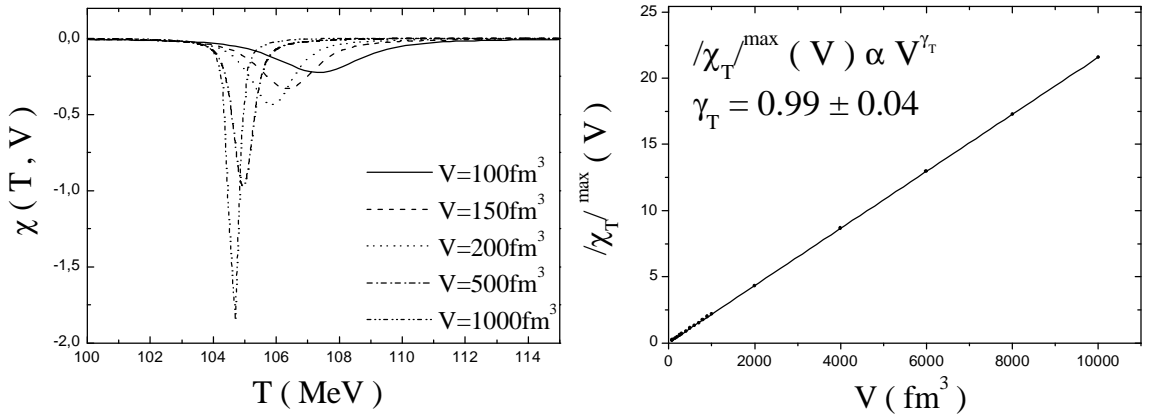


Fig. 4: (Left) Susceptibility $\chi(T, V)$ as a function of temperature for varying volume, and (Right) linear fit of the results for the maxima of the susceptibility vs volume.

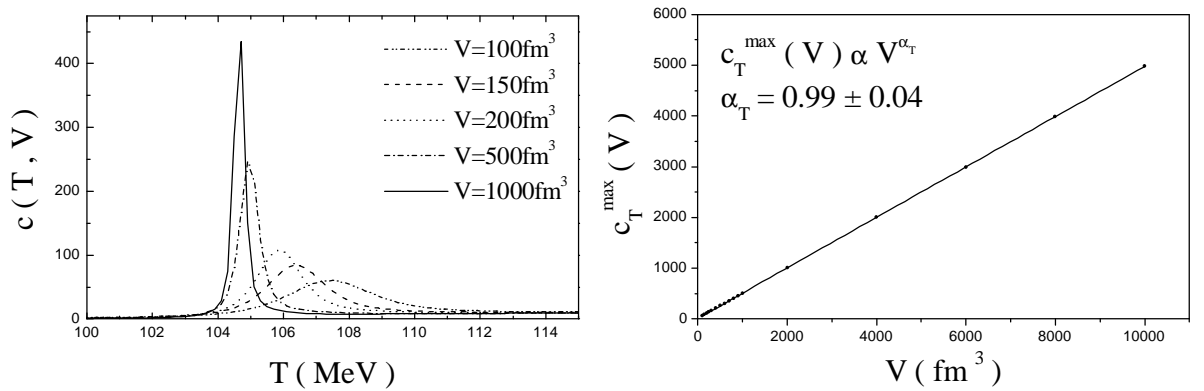


Fig. 5: Variations of (Left) the specific heat density with temperature for different system volumes and of (Right) the maxima of the specific heat density with the volume.

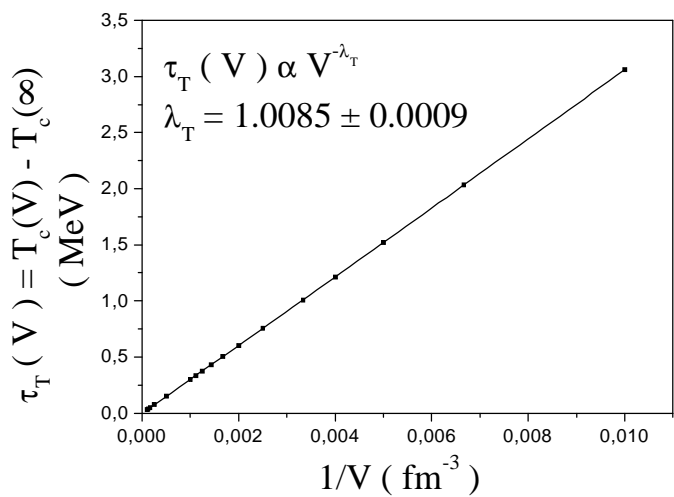


Fig. 6: Plot of the shift of the critical temperature vs inversed volume.

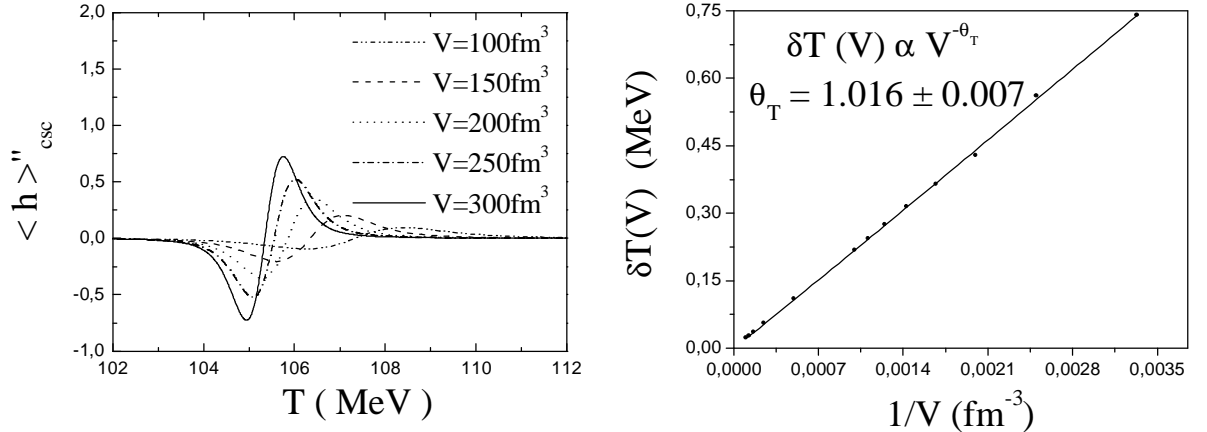


Fig. 7: (Left) Illustration of the second derivative of the order parameter $\langle h \rangle''_{\text{csc}} = \frac{\partial^2 \langle h(T,V) \rangle_{\text{csc}}}{\partial T^2}$ vs temperature, taken at different volumes. (Right) Data of the width of the temperature region over which the transition is smeared, fitted to a power-law of the inverse volume.